# Inflation Pressure Effects in the Nondimensional Tire Model

**Edward M. Kasprzak**
University at Buffalo

**Kemper E. Lewis**
University at Buffalo

**Douglas L. Milliken**
Milliken Research Associates, Inc.

## ABSTRACT

Inflation pressure affects every aspect of tire performance. Most tire models, including the Radt/Milliken Nondimensional Tire Model, are restricted to modeling a single inflation pressure at a time. This is a reasonable limitation, in that the Nondimensional model forms an input/output relationship between tire operating conditions and force & moment outputs. Traditional operating conditions are normal load, slip angle, inclination angle, slip ratio and road surface friction coefficient.

Tire pressure is more like a tire parameter than a tire operating condition. Since the Nondimensional Tire Model is semi-empirical it does not specifically deal with tire parameters like sidewall height or tread compound. Still, tire pressure is the easiest tire parameter to change, and as the air temperature within the tire varies during use so does the inflation pressure. Thus, it is desirable to incorporate inflation pressure into the Nondimensional Tire Model as an input.

This paper discusses the effects of tire pressure on tire force and moment output. Effects on lateral force and aligning torque are investigated in detail. Additionally, the effects on cornering stiffness, friction coefficients, peak aligning torque coefficient and peak shape are reviewed. New techniques to implement pressure effects in the Nondimensional Model are presented. Applications of these techniques are shown on a Formula SAE tire and a full-size radial racing tire.

Additionally, the effects of inflation pressure on tire spring rate and loaded radius are investigated. While these are not modeled using Nondimensional techniques, they are important variables accompanying any tire model.

## INTRODUCTION

A variety of tire models are in use around the world with various levels of complexity, scope and purpose. They can be based on detailed tire structural models, often employing finite element calculations, or they can be semi-empirical in nature. Applications range from tire ride modeling, envelopment of road surface irregularities, tread shape analysis, rolling resistance calculations, tire dynamics, tire force & moment prediction and beyond. All tire models have their own strengths and weaknesses, and applications to which they are well-suited.

The Radt/Milliken Nondimensional Tire Model is a semi-empirical tire model used to predict net tire forces and moments. By semi-empirical, we mean that the model combines known operating conditions with assumptions about tire behavior to predict tire force and moment outputs [1]. This paper follows SAE naming and axis system conventions as defined in [2]. Figure 1, repeated from [2], defines the tire axis system and many of the terms used throughout this paper.

Traditional inputs to the Nondimensional Model are:

$\alpha$      Slip Angle (deg, rad)

$\gamma$      Inclination Angle (deg, rad)

$\sigma$      Slip Ratio (unitless)

$F_z$      Normal Load (lb, N)

$\mu_S$      Surface Friction Coefficient (unitless)
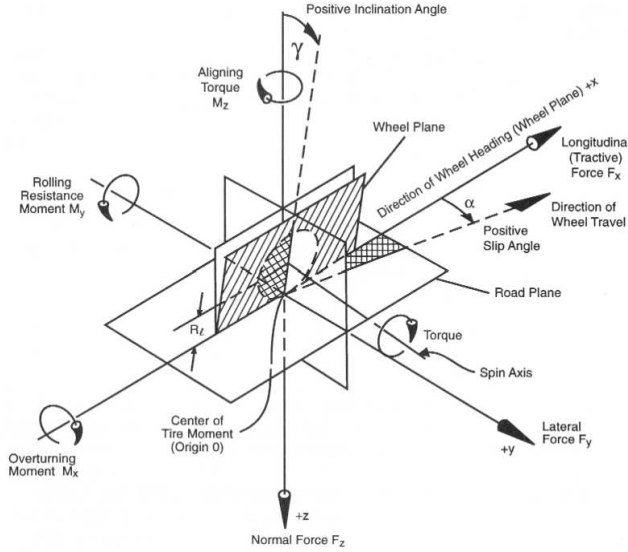
Figure 1. The tire coordinate system, definition of terms

Force and moment outputs are:

$F_y$      Lateral Force (lb, N)

$F_x$      Longitudinal Force (lb, N)

$M_z$      Aligning Torque (lb-ft, N-m)

$M_x$      Overturning Moment (lb-ft, N-m)

The Nondimensional Tire Model takes a unique approach to modeling tire data. It applies transformations to raw tire data, resulting in dimensionless variables. When a nondimensional output variable is plotted against a nondimensional input variable a single load- and friction-independent curve results. Radt and Milliken first proposed the Nondimensional model in 1960 [3]. They used Fiala's structural tire model [4] as the basis for development of the nondimensional transformations. In the simplest case, lateral force as a function of slip angle, the transformations are:

$$\bar{\alpha} = \frac{C \tan \alpha}{\mu F_z} \qquad (1)$$

$$\bar{F} = \frac{F_y}{\mu F_z} \qquad (2)$$

where $C$ is the cornering stiffness and $\mu$ is the ratio of peak lateral force to normal load at a given normal load. The nondimensional variables $\bar{\alpha}$ and $\bar{F}$ are unitless. In these transformations, $C$ and $\mu$ are not constants, but rather are themselves functions of the tire operating

conditions and, thus, functions of the inputs to the Nondimensional model.

Cornering stiffness is defined as:

$$C = \left. \frac{\partial F_y}{\partial \alpha} \right|_{\alpha=0} \qquad (3)$$

And is modeled as:

$$C = f(F_z) \qquad (4)$$

Friction Coefficient is defined as:

$$\mu = \left. \frac{F_y}{F_z} \right|_{\text{peak } F_y} \qquad (5)$$

And is modeled as:

$$\mu = f(F_z) \qquad (6)$$

While the peak of the lateral force curve happens at varying values of slip angle, slip angle is not required to be an argument to the function modeling friction coefficient. In this simplest case we are assuming a constant inclination angle, so the inclination angle does not appear in any of the above equations.

Variations of cornering stiffness and friction coefficient with load are assumed to be smooth and continuous. Raw data validates this assumption. Implementation of Equations 4 and 6 is typically accomplished using low-degree polynomials. A quadratic or cubic fit is usually sufficient.

In general, Figures 2 and 3 from Milliken/Milliken [5] show typical lateral force vs. slip angle curves and their subsequent transformation into nondimensional coordinates.
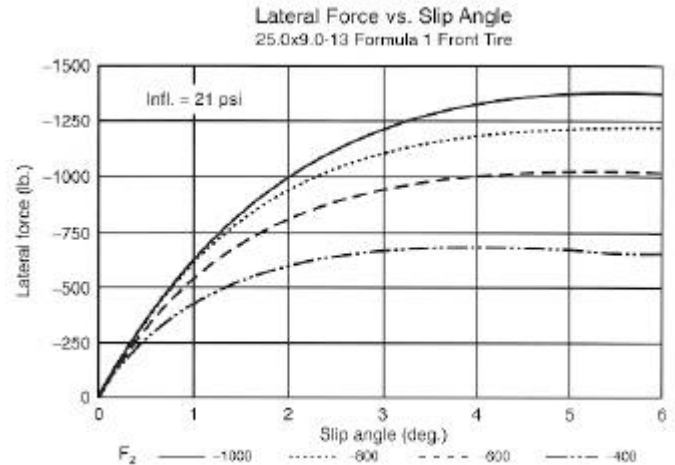
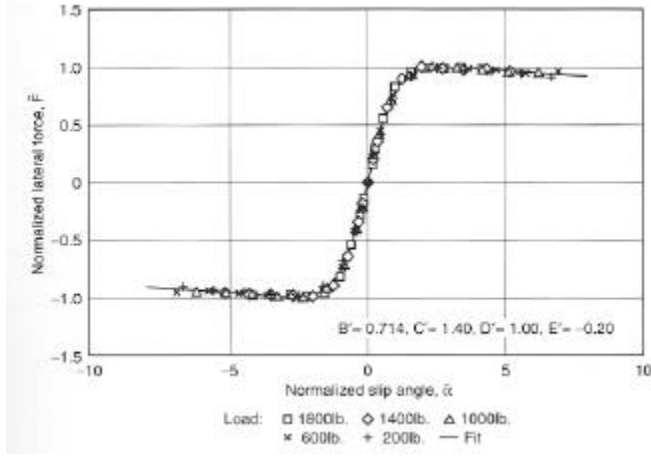

Figure 2. Typical Lateral Force vs. Slip Angle curves

Figure 3. Textbook Nondimensional lateral force vs. slip angle

The resulting load-independent curve in nondimensional coordinates (Figure 3) can then be fit by a functional relationship, $\bar{F} = f(\bar{\alpha})$. Early on, this was also based on the work of Fiala [4], such that $\bar{F}$ was a polynomial function of $\bar{\alpha}$. A significant improvement came in the mid-1980s when Bakker and Pacejka introduced the "Magic Formula" [6]. While Pacejka was using this "Magic Formula" to describe individual load curves, Radt and Milliken applied it to the single, compressed curve in nondimensional coordinates [5] with much success.

Equations 1 and 2 are the simplest in the family of nondimensional transformations. Other transformations exist which accommodate additional input variables and/or pertain to different force /moment outputs. For example, the transformation for the Nondimensional Slip Parameter $\bar{\beta}$ (an extension of the nondimensional slip angle $\bar{\alpha}$ of Equation 1) which allows for variations in inclination angle is:

$$\bar{\beta} = \frac{\bar{\alpha}}{1 - \bar{\gamma}\,\mathrm{sgn}\,\alpha} \tag{7}$$

where $\bar{\alpha}$ is defined in Equation 1 and the nondimensional inclination angle $\bar{\gamma}$ is defined as:

$$\bar{\gamma} = \frac{G\sin\gamma}{\mu F_z} \tag{8}$$

G is the camber stiffness, defined as:

$$G = \left.\frac{\partial F_y}{\partial \gamma}\right|_{\alpha=0} \tag{9}$$

And is modeled with a low-degree polynomial as:

$$G = f(F_z) \tag{10}$$

A good introduction to the Radt/Milliken Nondimensional Tire Model for several cases is given in Chapter 14 of Milliken/Milliken [5]. A more detailed summary is provided by Radt/Glemming [7]. Longitudinal force as a function of slip ratio is described, as are transformations for aligning torque, overturning moment, and pairs of the input variables slip angle, inclination angle and slip ratio. Preliminary work on the addition of inflation pressure to the Nondimensional Tire Model was previously discussed by Kasprzak in [8].

**OVERVIEW OF INFLATION PRESSURE EFFECTS**

Changing inflation pressure affects tire force and moment characteristics. This is because changes in inflation pressure alter the size, shape and contact pressure distribution in the footprint of the tire. In general, increasing inflation pressure will cause the size of the footprint to shrink, raise the contact pressure near the center of the footprint and allow less tire distortion (less footprint shape change).

Since the Nondimensional Tire Model is semi-empirical in nature, understanding the details of these effects is not critical. Instead, raw data generated on a tire testing machine at different inflation pressures is sufficient to draw some general conclusions and apply the model.

Raw data presented in this paper comes from two sources. The first is a 13 in. Formula SAE racing tire. This data was collected by the Formula SAE Tire Testing Consortium (FSAE TTC) [9] at the Calspan Tire Research Facility [10]. The second set of raw data was measured on a recent, full-size, radial racing tire. It is provided by Milliken Research Associates [11] and was also collected at Calspan TIRF.

During the development we will only present plots from the Formula SAE tire. Plots from the radial racing tire will be presented in a separate section. Figures 4, 5 and 6 show plots of lateral force and aligning torque for the Formula SAE tire. The following are common to these plots:

- Normal loads: 150 lb., 350 lb.
- Inclination Angle: 0 deg.
- Inflation Pressures, psi: 8 (blue), 10 (green), 12 (red), 14 (cyan), 16 (magenta)

In each of the figures, two distinct groups of five curves are identifiable. Each group represents one normal load, with one pressure per curve.
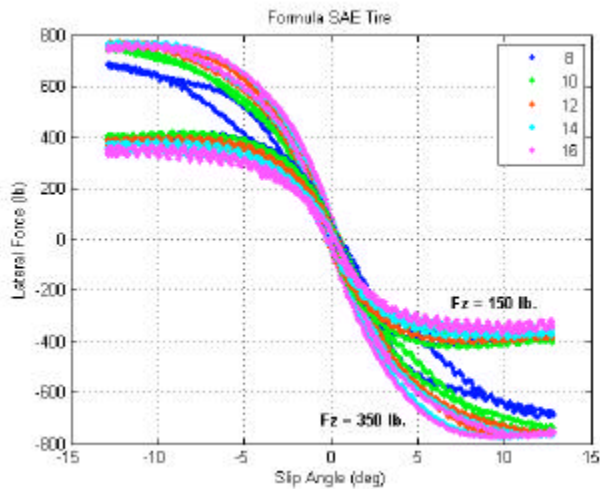
Figure 4.  Pressure Effect on Lateral Force
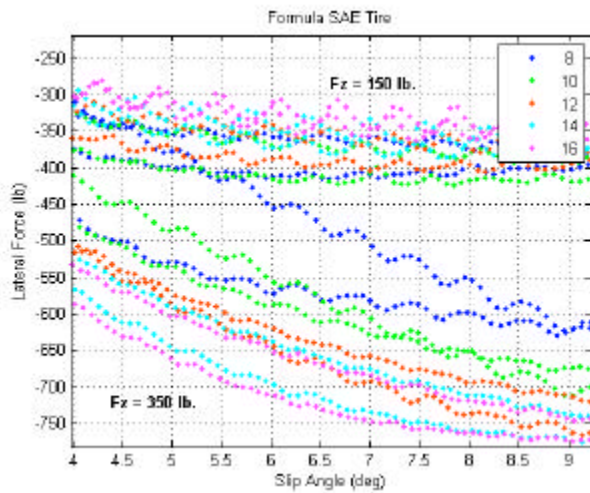


Figure 5.  Closer look at pressure effect on lateral force
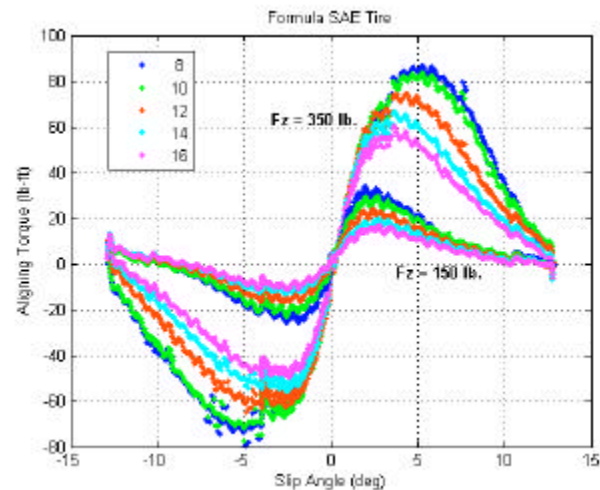


Figure 6.   Pressure Effect on Aligning Torque

Figure 5 shows a close-up of the lateral force curves seen in Figure 4.  From this figure a few comments on the recorded data can be made.  Each constant-load curve exhibits some amount of noise and hysteresis.  This is typical of measured tire data.  The hysteresis is a result of variables which cannot be controlled directly on the test platform, such as tread temperature.  Every measurement includes noise, and the high-frequency oscillatory behavior could be due to tire nonuniformities, an out-of-round wheel or the sampling instrument's built-in filtering algorithm.  These artifacts can be safely ignored for the work presented in this paper.

It is clear in all the figures that changing inflation pressure alters the force and moment curves.  In Figure 5 at 150 lb. normal load, a decrease in inflation pressure increases the lateral force capability of the tire.  In the slip angle range shown, the difference between 16 psi and 8 psi is approximately 40 lb. of lateral force.  This is a 10% difference.  At the 350 lb. load the effect of pressure is just the opposite.  Here lateral force capability increases as inflation pressure increases.  In the region shown, lateral force exhibits up to a 20% difference between 8 psi and 16 psi.

No drive/brake data was collected at various pressures on the Formula SAE tire, although the same techniques presented here can also be applied to longitudinal force.  In general, optimum longitudinal force performance occurs at lower inflation pressures.  Lateral and longitudinal forces are optimized at different pressures, and the trends often go in opposite directions (increasing inflation pressure typically increases lateral force capability but reduces longitudinal force capability).  This makes selecting tire pressures for a race car a very difficult compromise, as ideally we would like both lateral and longitudinal force capability to be optimized at the same pressure.

Figure 6 demonstrates the effect of inflation pressure on aligning torque.  As load increases, the effect of inflation pressure also increases—the range of values in the 150 lb. curve are much smaller than in the 350 lb. curve.  Unlike lateral force, however, the trend is always in the same direction.  Increasing inflation pressure reduces aligning torque which, when fitted to a car, reduces the steering effort and rigid body aligning torque.

From these sample plots it can be seen that inflation pressure has a noticeable effect on tire force and moment curves.  As such, adjustment of inflation pressure is an effective way to modify tire (and thus vehicle) performance.  Furthermore, inflation pressure increases as the contained air temperature increases with tire use.  This pressure "build-up" necessarily changes tire force and moment characteristics and must be accounted for when selecting initial or "cold" inflation pressures.  For these reasons it is highly desirable to have inflation pressure as an input to a tire model along with the traditional operating condition inputs.

## INFLATION PRESSURE AS AN INPUT VARIABLE

A literature review shows that there has been little published on incorporating pressure as an input to tire models. Prior to the work presented in this paper, the Nondimensional model could only be applied to data collected at a single pressure. If data was available at multiple pressures, each pressure would be fit with its own Nondimensional model.

Values at intermediate pressures could be predicted from a series of single-pressure models using several techniques. The simplest is to directly interpolate between the two nearest pressures. If linear interpolation is used, slope discontinuities across inflation pressure will appear at each measured pressure. Alternatively, force and moment values could be predicted at a given operating point for every pressure at which a model was developed. This could then be fit with a spline or a polynomial to determine values at intermediate pressures. While this technique often gives reasonable results, it is not consistent with the Nondimensional Tire Model approach.

The key feature of the Nondimensional model is its use of transformations based on physically-meaningful engineering quantities to compress tire data into load and friction independent curves. Post-expansion fitting of a polynomial or spline does not give any understanding of pressure effects on a fundamental level and reduces the accuracy of the model.

The correct Nondimensional approach is to include pressure in the transformations such as those shown in Equations 1 and 2. Development of this approach is given in the next section where, for simplicity, we focus only on lateral force at a constant inclination angle.

## LATERAL FORCE

Several approaches were considered before it was determined that the best way to incorporate pressure in Equations 1 and 2 was through the definitions of cornering stiffness and friction coefficient given in Equations 4 and 6. These equations now become:

$$C = f(F_z, P) \qquad (11)$$

$$\mu = f(F_z, P) \qquad (12)$$

where P is the inflation pressure. Figures 7 and 8 show the effect of inflation pressure on cornering stiffness and friction coefficient, respectively, for the Formula SAE tire lateral force curves shown previously in Figure 4.

In each of these figures the blue points are the values calculated from the raw data at each inflation pressure. The black line is a polynomial fit describing the inflation pressure effect at each load.
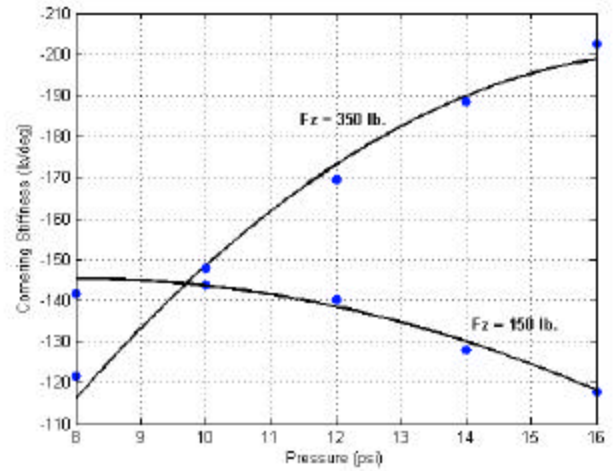


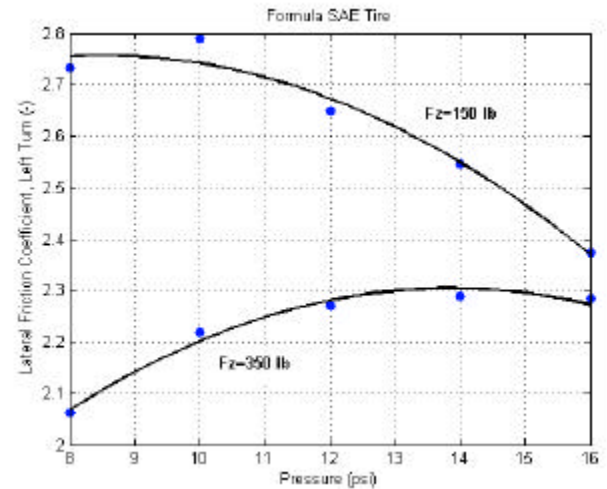Figure 7. Pressure effect on cornering stiffness



Figure 8. Pressure effect on friction coefficient

Prior to the addition of inflation pressure as an input, both friction coefficient and cornering stiffness were already modeled as functions of normal load (for this simplest case of constant inclination angle). The inclusion of inflation pressure means that these quantities must now be modeled as a response surface—functions of both normal load and pressure. A low-degree (cubic or less) polynomial response surface is often sufficient. Figures 17 and 18 presented later in the radial racing tire study present examples of these response surfaces. They are a better representation as there are more loads tested on the radial racing tire than the two loads available on the Formula SAE tire currently being presented.

The use of response surfaces to capture the effects of inflation pressure on cornering stiffness and friction

coefficient is sufficient to make the transformations in Equations 1 and 2 quite useful. Application of these transformations on the Formula SAE tire results in Figure 9. Here, all pressures and loads shown in Figure 4 are represented. As is the goal of the Nondimensional model, they all fall on a single curve.
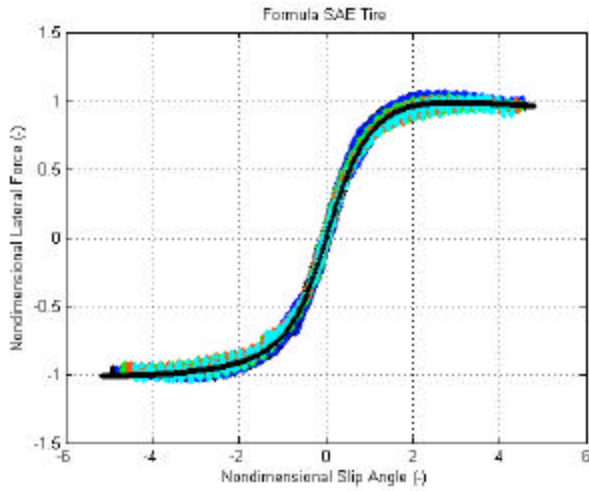


Figure 9. Nondimensional lateral force curve

This curve looks very similar to the textbook version presented in Figure 3. A single instance of the Magic Formula (black line) can be fit to this nondimensional curve.

This completes the Nondimensional model for the case of lateral force as a function of slip angle and inflation pressure. The transformations and single Magic Formula can now be used to expand the model at any operating point. The expansion is plotted against the raw data in Figure 10. This figure shows that the variations in lateral force with inflation pressure are adequately captured by the method described above.
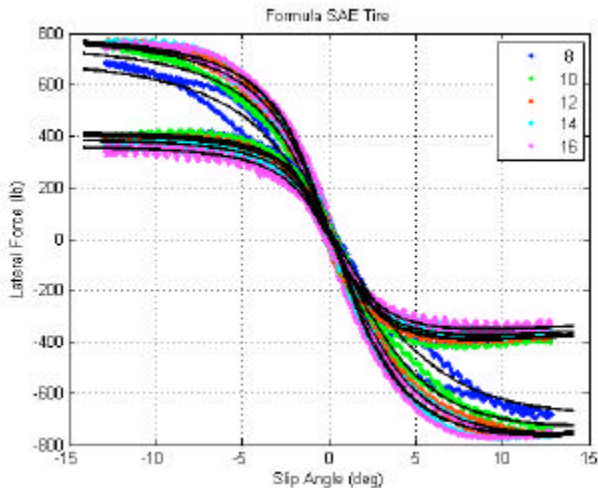


Figure 10. Expanded Nondimensional model, lateral force

## ALIGNING TORQUE

The approach to fitting aligning torque, $M_z$, as a function of slip angle and inflation pressure is analogous to that for lateral force. The transformation for slip angle is the same as Equation 1. The remainder of the relevant equations are:

$$\bar{F} = \frac{M_z}{\mu_{M_z} F_z} \tag{13}$$

$$C_{M_z} = \left. \frac{\partial M_z}{\partial \alpha} \right|_{\alpha=0} \tag{14}$$

$$\mu_{M_z} = \left. \frac{M_z}{F_z} \right|_{\text{peak } M_z} \tag{15}$$

$C_{M_z}$ and $\mu_{M_z}$ are the aligning stiffness and peak aligning torque coefficient, respectively. They are modeled as response surfaces:

$$C_{M_z} = f\left(F_z, P\right) \tag{16}$$

$$\mu_{M_z} = f\left(F_z, P\right) \tag{17}$$

Working with the data presented in Figure 6, these two quantities vary as shown in Figures 11 and 12. Again, this variation is captured in a low-degree (cubic or less) polynomic response surface across normal load and inflation pressure, although it is not shown here.

Application of the transformations leads to the compressed (nondimensional) curve shown in Figure 13. All combinations of normal load and inflation pressure are compressed to a single curve and a single instance of the Magic Formula represents this curve well. Expansion of the model leads to the curves shown in Figure 14.
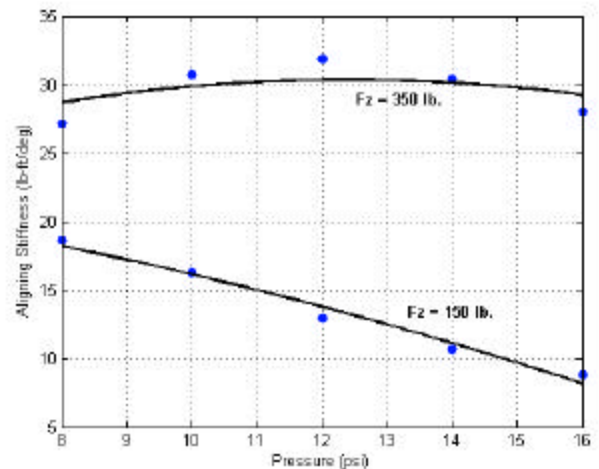


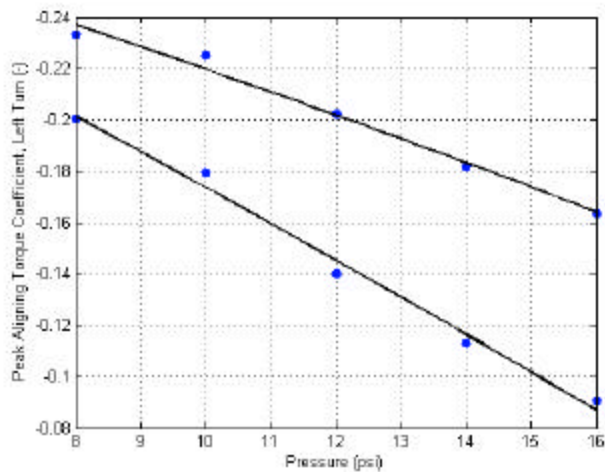Figure 11. Pressure effect on aligning stiffness

Figure 12.  Pressure effect on peak aligning torque coefficient
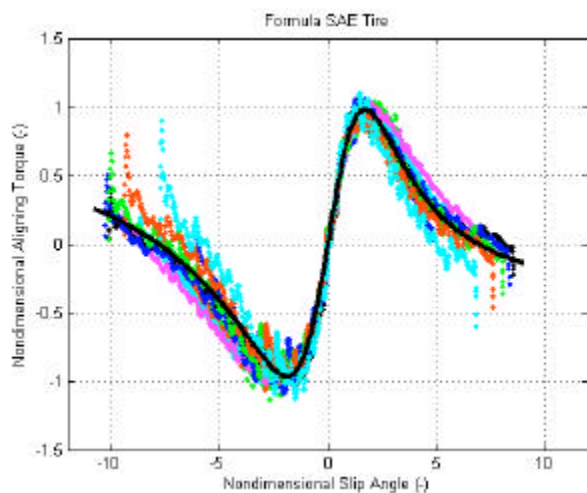


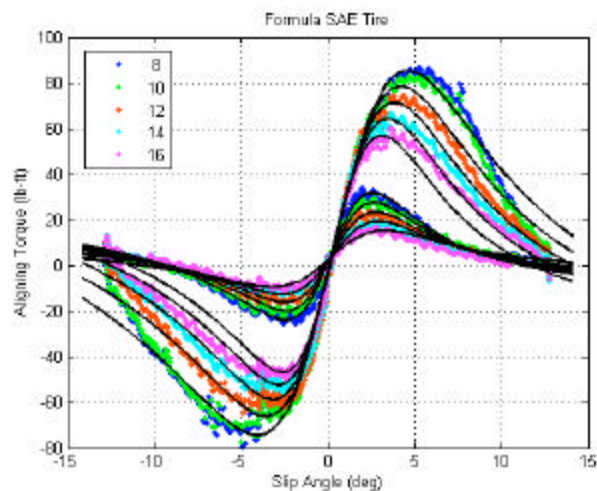Figure 13.  Nondimensional aligning torque curve



Figure 14.  Expanded Nondimensional model, aligning torque

On the whole the model fits the data well.  Past-peak model behavior deviates from the raw data at the higher load.  This will be addressed in the section on peak shape representation.

As can be seen in these figures, the Nondimensional technique does a good job accounting for inflation pressure effects on aligning torque.  In the next section we demonstrate applications of the same techniques presented for lateral force and aligning torque on a full-size radial racing tire.

## APPLICATION TO  A RADIAL RACING TIRE

As mentioned previously, Calspan data on a recent radial racing tire was provided by Milliken Research Associates, Inc.  The data collected is similar in structure to the Formula SAE tire data presented in the previous sections.  The main differences are the increased number of loads and the wider range of pressures for which data is available.  Five loads were tested: 200, 600, 1000, 1400 and 1800 lb.  Four pressures were tested:  20, 26, 32 and 38 psi.

Figure 15 shows lateral force plotted as a function of slip angle.  The five groups of lines correspond to the five normal loads tested.  Within each group the four pressures are each represented by a different color.  The result of the Nondimensional model is also seen on this graph—one line per combination of load and inflation pressure.  On the whole it can be seen that the techniques presented above to capture inflation pressure effects represent the data well.

Figure 16 shows a more detailed view of the high-load, left hand turn portion of Figure 15.  From this it can be seen that while the Nondimensional model generally captures the pressure effects there are definite deficiencies, especially at the highest load.  Techniques to address this will be presented in the next section.
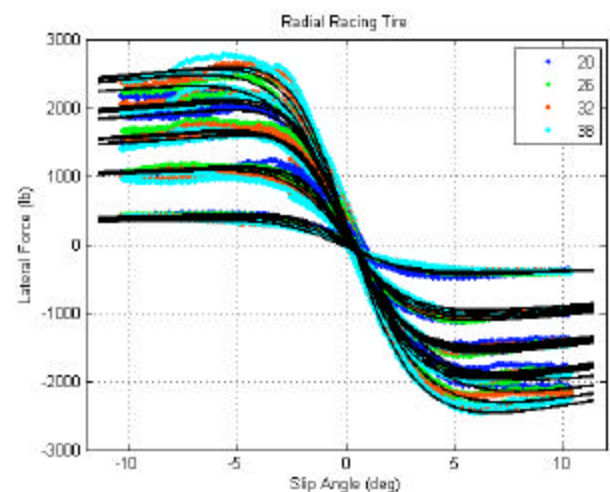


Figure 15.  Nondimensional model, lateral force, radial racing tire
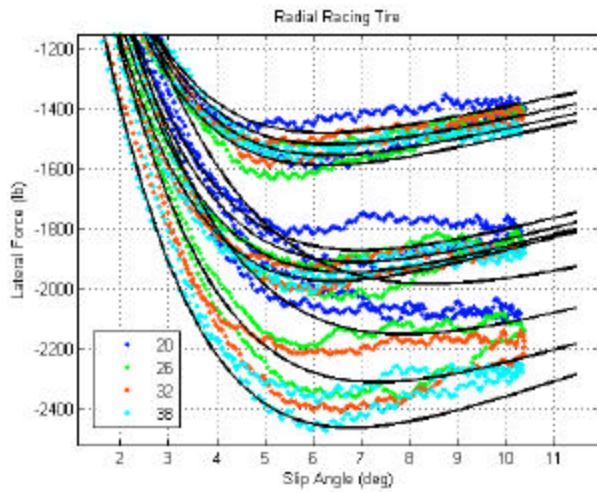
Figure 16. Left-hand turn, high load focus, lateral force, radial racing tire
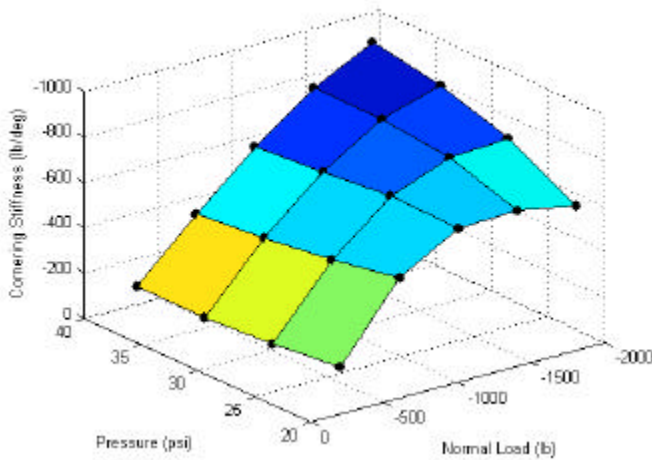


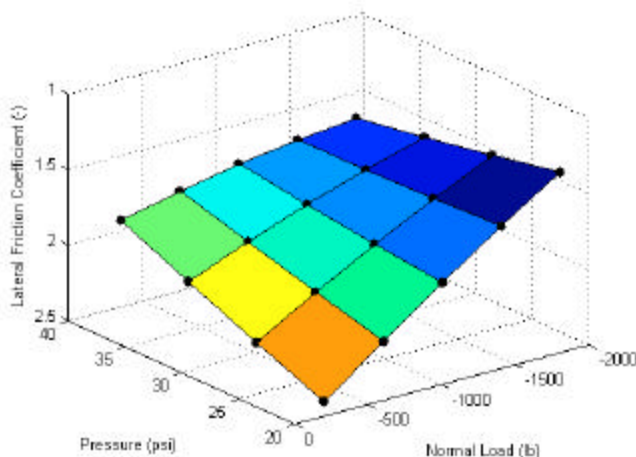Figure 17. Cornering stiffness variation with load and inflation pressure



Figure 18. Friction coefficient variation with load and inflation pressure

Because a larger number of loads were tested, the radial racing tire is a better platform to show the response surface implementation described by Equations 4 and 6. These are shown in Figures 17 and 18. Here, cornering stiffness and friction coefficient are seen to vary as a function of both normal load and inclination angle. This behavior is captured by response surfaces. Typically the response surface does not need to contain anything higher than a third degree term.

These results are typical of the Radt/Milliken Nondimensional tire model, and, while not shown, the aligning torque fits on the radial racing tire are similar to those generated for the Formula SAE tire.

## PEAK SHAPE REPRESENTATION

Figures 14 and 16 show that, in some instances, the Nondimensional model has difficulty modeling the raw data near and past the peak of the data curve. The equations presented previously focus largely on the linear range of tire behavior and the magnitude of the peak. Traditional Nondimensional theory assumes the nondimensionalized data curves, such as those shown in Figures 9 and 13, can be represented by a single functional relationship. Indeed, this is the goal of the transformations—to compress data to a single curve in nondimensional coordinates.

Generally this is accomplished. However, there are instances where the shape of the nondimensional curves at the peak vary sufficiently that a single fit to the compressed curve does not adequately capture the tire's behavior. That is, changes in load, inflation pressure and other operating variables interact with the tire to change the characteristic shapes of the data curves in such a way that the transformations do not capture all the effects. When all the effects are not represented in the transformations the nondimensional space does not exhibit a compact, single curve.

An example of this behavior is shown in Figure 19. This is the same data presented in the radial racing tire section, leading to Figures 15 and 16. In this figure each color represents a unique combination of normal load and inflation pressure. While each combination generally falls on a single compressed curve, it can be seen that some combinations peak sooner than others and show more curvature at the peak than others. For example, compare the green and magenta curves. Figure 13 shows similar behavior for aligning torque.

As a result, fitting a single functional relationship through this collection of points will fail to capture all of the tire's characteristics, ultimately leading to inaccuracies in the expanded version of the model. Research is continuing on how to best-address this issue consistent with the Radt/Milliken Nondimensional Tire Model approach.
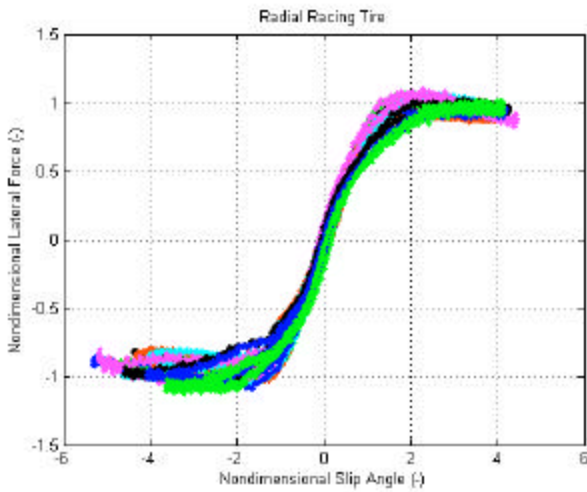
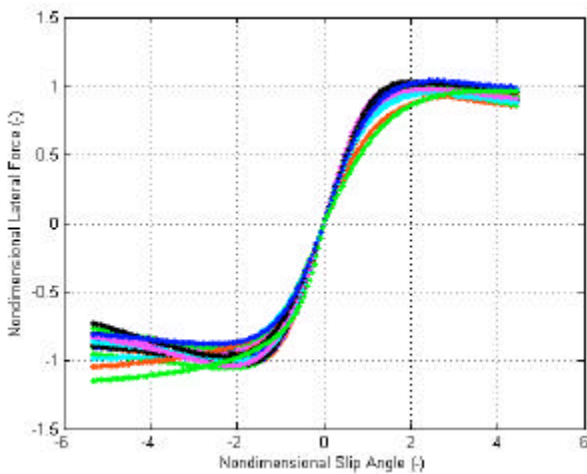Figure 19. Nondimensional curve with incomplete compression



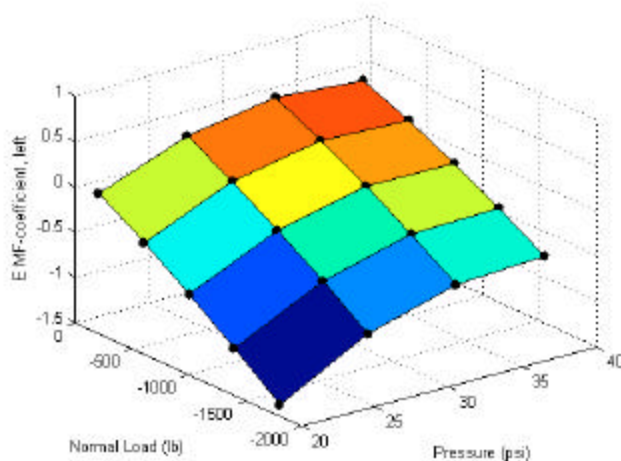Figure 20. Magic Formula fit of each load and pressure combination



Figure 21. Magic Formula "E" coefficient variation with load and pressure

In the meantime, a relatively simple and effective solution is proposed. Instead of fitting the curve in Figure 19 with a single instance of the Magic Formula, each combination of normal load and inflation pressure is fit with its own instance of the Magic Formula. In this case with five loads and four inflation pressures a total of 20 instances of the Magic Formula are determined. The resulting curves appear as shown in Figure 20, which highlight just how different the curve shapes in the Nondimensional space can be.

With coefficients for each individual Magic Formula curve determined, patterns in the way the coefficients vary as a function of the input variables can be identified. These have been found to vary smoothly and, as with cornering stiffness, friction coefficient and other parameters presented earlier, are well-described by low-degree (cubic or less) polynomic response surfaces. For example, Figure 21 illustrates the variation of the Magic Formula's "E" coefficient with normal load and inflation pressure. Response surfaces for the other coefficients are similar.

By allowing the Magic Formula coefficients to vary as a function of normal load and inflation pressure, effects not currently captured by the transformations can be represented. Figure 22 shows the improved fit for lateral force (compare with Figure 16). And Figure 23 presents an improved fit for aligning torque (compare with Figure 14). Note that the past-peak behavior is improved compared with Figures 14 and 16.

While the resulting model fits correspond well with the raw data, the technique is not consistent with the Nondimensional model approach. Since the effects are not captured in transformations but rather in a post-transformation modification the results cannot be scaled as accurately to surfaces of different friction coefficient. In instances where the resulting Nondimensional curve is described by a single instance of the Magic Formula expansions at different surface friction coefficient values are properly handled.
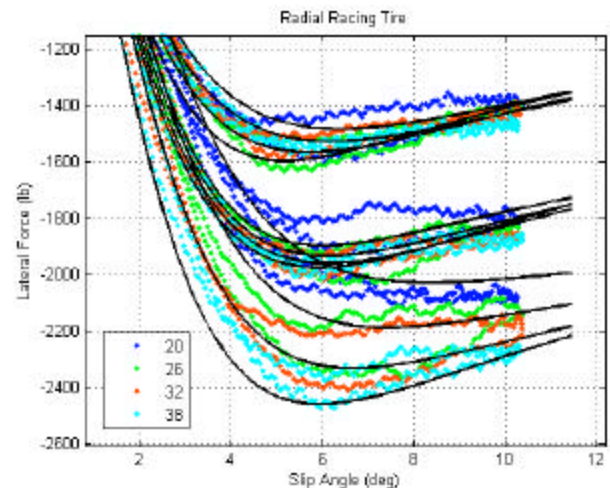


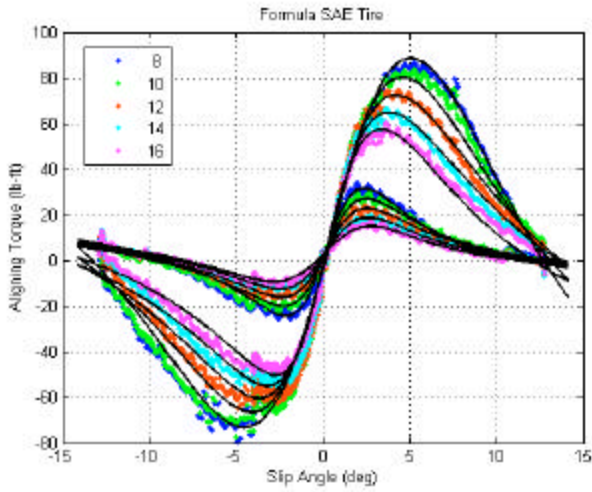Figure 22. Improved lateral force fit

Figure 23.  Improved aligning torque fit

That said, this hybrid approach does a very good job of representing the tire curves and can be used to capture tire characteristics not represented in the typical Nondimensional transformations.   Whether this approach will be replaced by more comprehensive transformation equations remains to be seen.  It is the subject of continuing research.

## OTHER CONDITIONS AND OUTPUTS

Techniques to incorporate inflation pressure effects into the Radt/Milliken Nondimensional Tire Model have been shown for lateral force and aligning torque at constant inclination angle.  While the transformations themselves have not been altered, the inflation pressure contribution to the transformations has been included through response surface descriptions of cornering stiffness, aligning stiffness, lateral friction coefficient and peak aligning torque coefficient.

The same technique has been applied to longitudinal force.   In this instance, the tractive stiffness and longitudinal friction coefficient are represented with response surfaces.  While not shown here, results are of the same quality as those presented above. Descriptions of the traditional longitudinal force transformations are found in Milliken/Milliken [5] and Radt/Glemming [7].

Radt/Glemming [7] also describe combined slip angle and inclination angle operation. Equations 7 through 10 summarize the transformations used to model lateral force as a function of this pair of inputs.  Addition of inflation pressure effects is accomplished in a similar way to the previous development when inclination angle was held constant.  Low-degree polynomic response surfaces are generated as a function of three variables:

$$C = f\left(F_z, \gamma, P\right) \tag{18}$$

$$G = f\left(F_z, \gamma, P\right) \tag{19}$$

$$\mu = f\left(F_z, \gamma, P\right) \tag{20}$$

In addition to affecting force and moment curves, inflation pressure changes also modify spring rate, loaded radius and effective radius characteristics. While these are not modeled with the same data-compressing techniques of the Nondimensional model, for completeness a review of these effects is presented here.

In general, tire vertical spring rate increases as inflation pressure is increased.  Sample data from a Formula SAE tire at a nominal load is shown in Figure 24.  The magnitude of this effect is significant.  For this tire the sensitivity is approximately 30 lb/in increase in spring rate per 1 psi increase in inflation pressure.   This variation is well-described by a cubic polynomial.
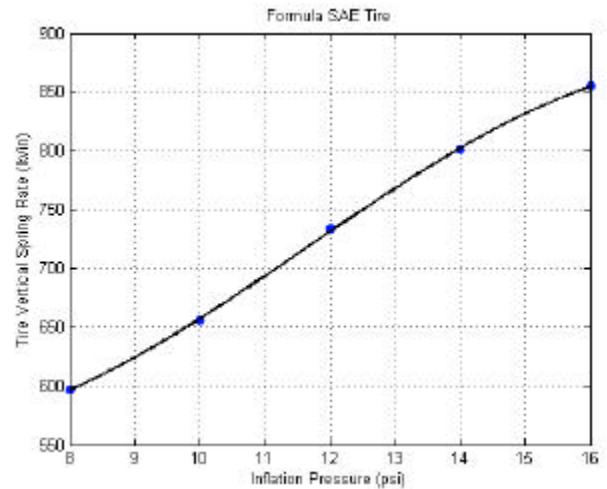


Figure 24.  Inflation pressure effect on spring rate

Since the tire spring rate acts in series with the suspension springs and dampers any changes in tire spring rate also affect load transfer, ride quality, ride heights, etc.  This can be an important consideration when control of body attitude is important to maintain a desired aerodynamic platform.

Figure 25 presents loaded radius data for the radial racing tire at a constant inclination angle, zero slip angle and zero slip ratio (all of which also affect the loaded radius).  As expected, the loaded radius is a strong function of normal load, but it is also a fairly strong function of inflation pressure.  This is especially true at high loads.
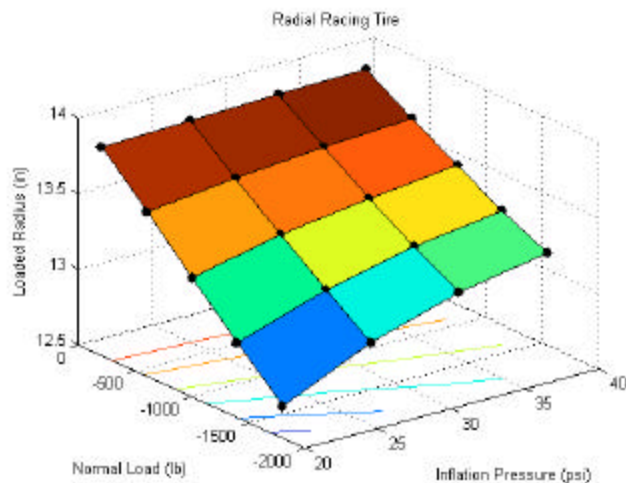
Figure 25. Inflation pressure effect on loaded radius

The lower right edge of the curve indicates that, at an 1800 lb. load, the loaded radius changes 0.5 inches over the range of pressures shown. This range of pressures is representative of the pressure build-up seen as tires heat during use. Thus, a cold tire at this load will be half an inch shorter than the same tire after it has been used for a number of laps and the inflation pressure has increased due to core air temperature increases. This has significant implications on ride height and body attitude.

## FUTURE WORK

This paper represents a significant step forward for the Nondimensional Tire Theory. Prior to this, inflation pressure effects had not been considered within the scope of the model. Furthermore, there was no way to account for peak shape variations in nondimensional data curves.

There are a few avenues of continuing research. First, while the pressure variations have been successfully modeled in cases of single inputs (slip angle) and pairs of inputs (e.g., slip angle and inclination angle), it has not been applied to the full case, namely combined non-zero slip angle, inclination angle and slip ratio. This most general operating condition has eluded nondimensionalization and is the subject of continuing research.

The peak shape variations in the nondimensional curves also require further research. Perhaps there are more comprehensive nondimensional transforms than the standard equations used since the Nondimensional Tire Theory was introduced. While Equations 1 and 2, for example, have been very successful in compressing data curves, the fact that they don't fully compress curves in some cases indicates that they do not capture some mechanism of tire behavior. In this paper this shortcoming has been removed by the new technique for post-nondimensionalization curve fitting. There may, however, be a more fundamental method for handling this behavior, one that modifies the transformation equations themselves to achieve complete compression of the data to a single curve. This, too, is an active area of continuing research.

## CONCLUSION

Through the techniques presented in this paper, the Radt/Milliken Nondimensional Tire Model has been extended to include inflation pressure as an operating variable. Inflation pressure has been shown to have significant effects on tire force and moment characteristics, as well as tire spring rate and loaded radius. The key to the technique is to capture inflation pressure effects in the same manner as normal load effects. Measured parameters used in the nondimensional transformations, such as cornering stiffness and friction coefficient, become functions of inflation pressure as well as normal load. As a multi-variable function, the behavior is best-represented by a response surface. Since tires exhibit continuous, smooth variation of these parameters with load and pressure, low-degree (cubic or less) polynomic response surfaces are sufficient.

This technique, in combination with the previously-existing nondimensional transformations does a good job of compressing raw data curves at several inflation pressures to a single curve in nondimensional coordinates. At times, tire response to pressure is such that the characteristic shape of the force and moment curves are altered, resulting in incomplete compression of the nondimensional curve. In these instances, applying a functional relationship at each combination of load and pressure, and then determining how the coefficients of this relationship vary with load and pressure, captures the variations. Once again, low-degree polynomic functions suffice to describe coefficient variation.

While research is continuing towards refining the effectiveness of the techniques used to capture inflation pressure effects, especially in the near-peak and past-peak regions, the approaches presented here show very good correlation with data collected on a Formula SAE tire and a radial racing tire.

## ACKNOWLEDGMENTS

# REFERENCES

1. Milliken, W.F., "High Camber Tests of Treaded and Smooth Motorcycle Tires on Calspan Tire Research Facility", January 1975.
2. SAE J670e, "Vehicle Dynamics Terminology". Society of Automotive Engineers, Inc., 400 Commonwealth Drive, Warrendale, PA 15096, June 1978.
3. Radt, H.S. and W.F. Milliken, "Motions of Skidding Automobiles", SAE Paper Number 205A, SAE Summer Meeting, Chicago, IL, June 5-10, 1960.
4. Fiala, E., "Seitenkrafte am Rollenden Luftreifen" ("Lateral Forces on Rolling Pneumatic Tires"), Zeitschrift, V.D.I., Vol. 96, No. 29, October 11, 1954, pp. 973-979.
5. Milliken, W.F. and D.L. Milliken, "Race Car Vehicle Dynamics", SAE International, Warrendale, PA, 1995.
6. Bakker, E., L. Nyborg and H.B. Pacejka, "Tire Modeling for Use in Vehicle Studies", SAE Paper No. 870421, SAE, Warrendale, PA, 1987.
7. Radt, H.S. and D.A. Glemming, "Normalization of Tire Force Moment Data", Tire Science and Technology, TSTCA, Vol. 21, No. 2, April-June, 1993, pp. 91-119.
8. Kasprzak, E.M., K.E. Lewis and D.L. Milliken, "Tire Asymmetries and Pressure Variations in the Radt/Milliken Nondimensional Tire Model", SAE Paper No. 2006-01-1968, SAE, Warrendale, PA, 2006.
9. Formula SAE Tire Testing Consortium, www.millikenresearch.com/fsaettc.html
10. Calspan Tire Research Facility, www.calspan.com/tire.htm
11. Milliken Research Associates, Inc. www.millikenresearch.com

## CONTACTS

Edward M. Kasprzak
Ph.D. candidate, University at Buffalo SUNY
Associate, Milliken Research Associates, Inc.
(716) 471-1742
kasprzak@eng.buffalo.edu